# Accepted Manuscript


Synthesis and evaluation of 6-(3-[$^{18}$F]fluoro-2-hydroxypropyl)-substituted 2-pyridylbenzothiophenes and 2-pyridylbenzothiazoles as potential PET tracers for imaging Aβ plaques

Byoung Se Lee, So Young Chu, Hye Rim Kwon, Chansoo Park, Uthaiwan Sirion, Damian Brockschnieder, Thomas Dyrks, Seung Jun Oh, Jae Seung Kim, Dae Yoon Chi

PII: S0968-0896(16)30182-1
DOI: http://dx.doi.org/10.1016/j.bmc.2016.03.034
Reference: BMC 12883

To appear in: *Bioorganic & Medicinal Chemistry*

Received Date: 31 January 2016
Revised Date: 17 March 2016
Accepted Date: 18 March 2016

Please cite this article as: Lee, B.S., Chu, S.Y., Kwon, H.R., Park, C., Sirion, U., Brockschnieder, D., Dyrks, T., Oh, S.J., Kim, J.S., Chi, D.Y., Synthesis and evaluation of 6-(3-[$^{18}$F]fluoro-2-hydroxypropyl)-substituted 2-pyridylbenzothiophenes and 2-pyridylbenzothiazoles as potential PET tracers for imaging Aβ plaques, *Bioorganic & Medicinal Chemistry* (2016), doi: http://dx.doi.org/10.1016/j.bmc.2016.03.034

# Synthesis and evaluation of 6-(3-[$^{18}$F]fluoro-2-hydroxypropyl)-substituted 2-pyridylbenzothiophenes and 2-pyridylbenzothiazoles as potential PET tracers for imaging Aβ plaques.

Byoung Se Lee [a], So Young Chu [a], Hye Rim Kwon [b], Chansoo Park [a], Uthaiwan Sirion [b, †], Damian Brockschnieder [c], Thomas Dyrks [c], Seung Jun Oh [d], Jae Seung Kim [d], Dae Yoon Chi [a,b,*]

[a] *Research Institute of Labeling, FutureChem Co., Ltd, Seoul 138-736, Korea*

[b] *Department of Chemistry, Sogang University, Seoul 121-742, Korea*

[c] *Global Drug Discovery - Molecular Imaging, Bayer Healthcare AG, 13353 Berlin, Germany*

[d] *Department of Nuclear Medicine, Asan Medical Center, University of Ulsan, College of Medicine, Seoul 138-736, Korea*

*** Corresponding author. Tel.: +82 2 715 2430; fax: +82 2 715 2411.**

E-mail address: dychi@sogang.ac.kr.

[†] Current address: Department of Chemistry and Center for Innovation in Chemistry, Faculty of Science, Burapha University, Sangsook, Chonburi 20131, Thailand.

*Keywords*: Alzheimer's disease (AD), β-Amyloid (Aβ), Positron Emission Tomography (PET)

**ABSTRACT**

3-[$^{18}$F]Fluoro-2-hydroxypropyl substituted compounds were synthesized and evaluated as novel $^{18}$F-labeled PET tracers for imaging Aβ plaque in a living brain. All compounds exhibited high binding affinities toward the synthetic $A\beta_{1-42}$ aggregate and/or Alzheimer's disease brain homogenate. In the microPET study with normal mice, the 3-[$^{18}$F]fluoro-2-hydroxypropyl substituted compounds resulted in fast brain washout by reducing the lipophilicities of the compounds. Intriguingly, (*S*)-configured PET tracers, (*S*)-[$^{18}$F]**1b** and (*S*)-[$^{18}$F]**1c**, exhibited a 2.8 and 4.0-fold faster brain washout rate at a peak/30 min in the mouse brain than the corresponding (*R*)-configured PET tracers despite there being no meaningful difference in binding affinities toward Aβ plaque. A further evaluation of (*S*)-[$^{18}$F]**1c** with healthy rhesus monkeys also revealed excellent clearance from the frontal cortex with ratios of 7.0, 16.0, 30.0 and 49.0 at a peak/30, 60, 90, and 120 min, respectively. These results suggest that (*S*)-[$^{18}$F]**1c** may be a potential PET tracer for imaging Aβ plaque in a living brain.

## 1. Introduction

The accumulation of Aβ plaque in the brain is believed to be the main origin of Alzheimer's disease (AD), which is the leading cause of dementia, accounting for 60-70% of all cases.[1] A positron emitting tracer that binds to Aβ plaque selectively offers an opportunity of the early detection of AD,[2] and will be useful for identifying new therapeutic drugs and monitoring the treatment results as a surrogate marker.[3] In 2002, $^{11}$C-labeled [$^{11}$C]PIB (Pittsburgh compound B) was developed for imaging Aβ plaque in the brain of living subjects by modifying Thioflavin T, which has been used as a fluorescent dye for staining Aβ plaque in postmortem brains.[4] [$^{11}$C]PIB

exhibited good Aβ plaque binding in a living brain with an appropriate brain accumulation and washout ratio. On the other hand, it is of limited use in clinical trials because the C-11 isotope has a half-life of only 20 min, which is too short to exhibit wide availability to AD patients from a single automated production. In this regard, many researchers have searched for longer lived F-18 (110 min half-life) labeled PET tracers for clinical use in the diagnosis of AD.[5] As a result, three F-18 labeled PET tracers have been approved by the U.S. Food and Drug Administration (FDA) in 2012 (Amyvid™, Eli Lilly),[6] 2013 (Vizamyl™, GE Healthcare),[7] and 2014 (Neuraceq™, Piramal)[8] as Aβ imaging agents and a secondary tool for the diagnosis of AD.

To be a good Aβ imaging PET tracer, it should meet two essential criteria in the stage of candidate discovery; selective binding toward Aβ plaque with high affinity and rapid clearance of non-specific binding from the brain.[9] Most biaryl and conjugated biaryl compounds have good binding affinities toward Aβ plaque in vitro.[10] On the other hand, many F-18 labeled biaryl candidates have failed to meet the desired washout criterion in vivo. The nucleophilic aliphatic [$^{18}$F]fluorination of alkyl tosylate or mesylate precursors is a common way to label the molecule of interest with F-18.[11] The resulting [$^{18}$F]fluoroalkyl substituents, however, play a key role increasing the lipophilicity of the molecules, giving rise to poor pharmacokinetic properties as well as undesirable non-specific interactions.

Our attempts have been made to find novel candidates suited to PET imaging of Aβ deposition considering these requirements. As an early our attempt (unpublished), 6-(3-[$^{18}$F]fluoropropyloxy)-2-(4-methylamino)phenyl benzo[*b*]thiophene ([$^{18}$F]FC028) was synthesized and evaluated by in vitro binding assay and in vivo biodistribution. Although it showed an excellent binding affinity of 0.27 nM ($K_i$) to Aβ aggregates compared to [$^{11}$C]PIB (0.78 nM), a biodistribution study with normal mice revealed low initial uptake (2.02 %ID at 2

min) and a poor washout effect (2.18 %ID at 30 min, and 3.14 %ID at 60 min), probably due to its high lipophilicity (CLogP = 5.31). The desired LogP for BBB penetration is believed to range from 1 to 3.[12] Subsequently, an effort was made to reduce the lipophilicity of the compound for better brain pharmacokinetics by modifying the core structure and functional groups. This paper describes how the introduction of a hydroxyl group and nitrogen atoms to the molecule affects the brain pharmacokinetics. More intriguingly, the large difference in brain pharmacokinetics between (*R*)- and (*S*)-enantiomers is also described.

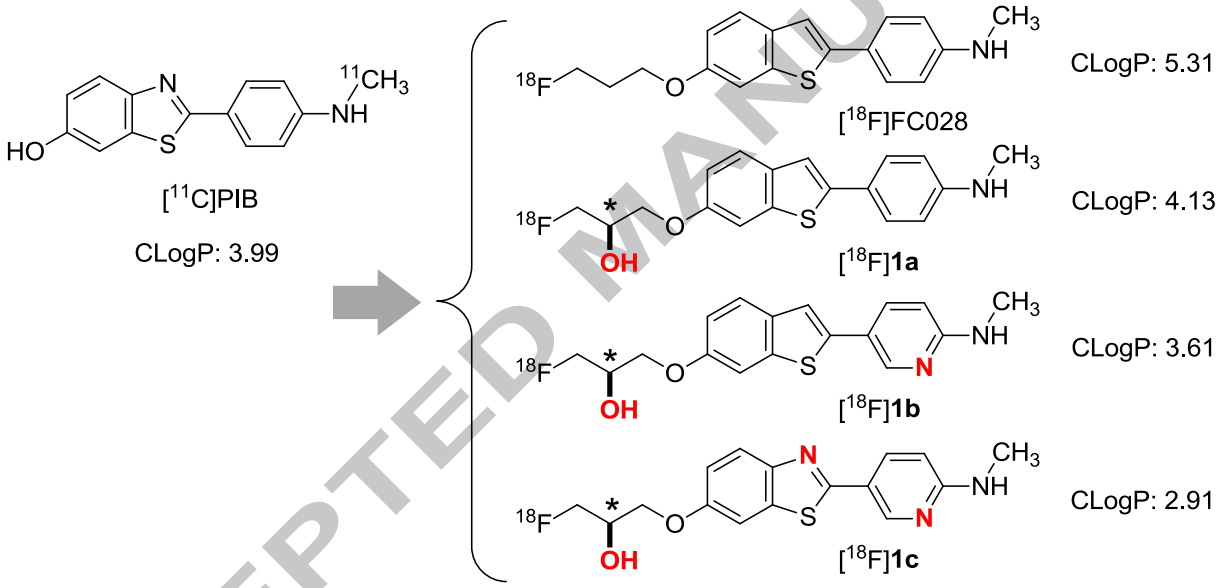


**Figure 1**. Structure modification and corresponding CLogP. The asterisk (*) indicates the stereogenic carbon. The red letters mean polar modifiers.

## 2. Results and discussion

### 2.1. Chemistry

A biaryl compound, 2-phenylbenzo[*b*]thiophene was chosen as the starting molecule, and the *N*-methylamino group on C4 position of the right ring was fixed. Two components, a nitrogen atom and hydroxyl group, were considered as polar modifiers to reduce the lipophilicity of the compounds (Figure 1). Nitrogen atoms were added to the phenyl and benzo[*b*]thiophene rings to become pyridine and benzo[*d*]thiazole rings, respectively. The pyridine ring was reported to reduce the level of non-specific white matter (no Aβ plaques region) binding compared to a phenyl ring.[13] The early developed F-18-labeled PET tracers (Amyvid™, Vizamyl™, and [$^{18}$F]Neuraceq™ [14]) have considerable non-specific white matter uptake compared to [$^{11}$C]PIB.[15] This white matter retention may limit the detection sensitivity of Aβ plaque, particularly in the prodromal phase of AD. The simple combination of pyridine and either benzo[*b*]thiophene or benzo[*d*]thiazole rings gave 2-pyridyl-benzo[*b*]thiophene and benzo[*d*]thiazole, as shown in Figure 1.

In addition, a hydroxyl group was introduced to the 3-fluoropropyl chain to reduce the unwanted lipophilicity caused by the 3-fluoropropyl substituent. Based on the CLogP value,[16] the hydroxyl group might be effective in offsetting the additional lipophilicity of the 3-fluoropropyl group. As a consequence of the structural modification, the CLogP value was found to decrease by up to 2.91, which is suited to BBB penetration. Note that the secondary hydroxyl group provides two enantiomers.

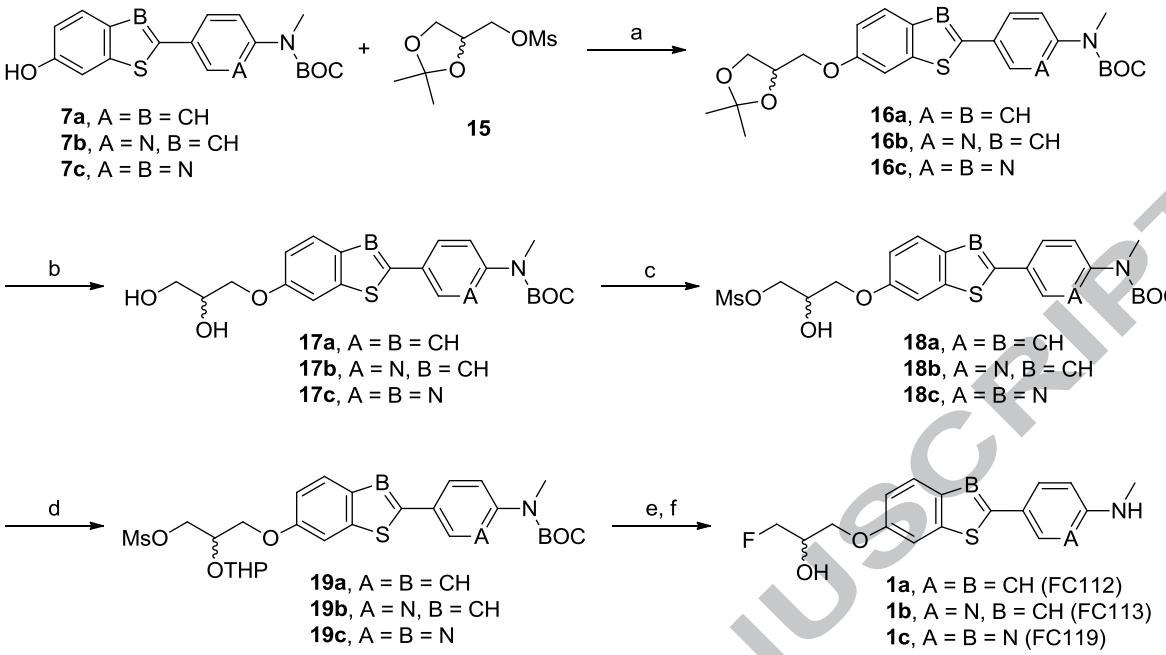


**Scheme 1**. Synthesis of 3-fluoro-2-hydroxypropyl substituted compounds. Reagents and conditions: (a) $Cs_2CO_3$, DMF, 100 °C, 1 h; (b) Dowex 50WX2, 10% $H_2O$/MeOH, 40 °C, 24 h; (c) MsCl, DIPEA, $CH_2Cl_2$, -10 °C, 30 min; (d) DHP, PPTS, $CH_2Cl_2$, rt, 17 h; (e) TBAF, *t*-amyl alcohol, 100 °C, 6 h; (f) 4 N HCl, 80 °C, 30 min.

Scheme 1 outlines the synthesis of 3-fluoro-2-hydroxypropyl substituted compounds **1a-1c**. The *O*-Alkylation of 6-hydroxy compounds **7a-7c** with 2,3-isopropylideneglycerol methanesulfonate (**15**) was carried out using $Cs_2CO_3$ at 80 °C overnight, in which compound **15** was a *R*/*S* racemate (see supplementary data for detail synthesis of **7a-7c**). The selective deprotection of the acetonide moiety was achieved using Dowex 50WX2 resin (hydrogen form) with careful monitoring by TLC, affording 1,2-diol compounds **17a-17c**.[17] The primary alcohol was treated with methanesulfonyl chloride (MsCl) and diisopropylethylamine (DIPEA), and the secondary alcohol was then tetrahydropyranylated in the presence of pyridinium *p*-

toluenesulfonate (PPTS) to give compounds **19a-19c**, respectively. The resulting *N*-Boc and *O*-THP protected mesylate compounds **19a-19c** were used as precursors for the synthesis of the F-18 labeled radioligands. The cold authentic compounds **1a-1c** were prepared as a racemate by the nucleophilic displacement of the mesylate leaving group of compounds **19a-19c** with tetra-*n*-butylammonium fluoride (TBAF) in *t*-amyl alcohol solvent[18] and the subsequent deprotection of *N*-Boc and *O*-THP under acidic conditions. Enantiomerically pure compounds and mesylate precursors were also prepared. They could be obtained from optically pure (*S*)- or (*R*)-2,3-isopropylideneglycerol methanesulfonate (**15**, 99 ee% each) using the same procedure as Scheme 1. Synthesis with (*S*)-2,3-isopropylideneglycerol methanesulfonate ((*S*)-**15**) provided the (*R*)-configured compound (*R*)-**1**, and synthesis with (*R*)-2,3-isopropylideneglycerol methanesulfonate ((*R*)-**15**) provided the (*S*)-configured compound (*S*)-**1**. Figure 2 shows the stereochemical structures, in which *R* and *S* indicate the absolute configuration on the hydroxyl group-attached carbon.

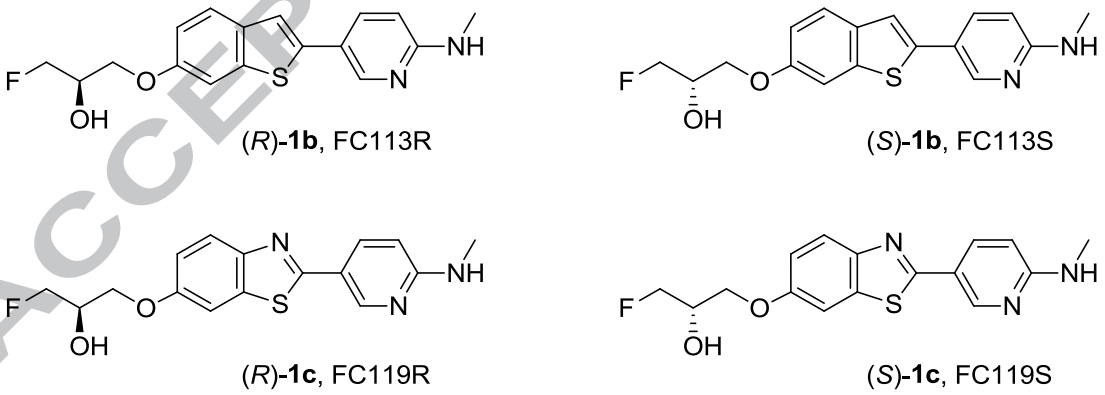


**Figure 2**. (*R*)- and (*S*)-Configured compounds.

### 2.2. Binding assay

A binding study was performed in two ways using synthetic $A\beta_{1-42}$ protein aggregate and AD brain homogenate. Cold PIB and florbetaben (Neuraceq™, formerly, AV-1) were also examined for comparison. A competition binding experiment was carried out first using synthetic $A\beta_{1-42}$ protein aggregate in the presence of 6-[$^{125}$I]iodo-2-(4-dimethylaminophenyl)benzo[*d*]thiazole ([$^{125}$I]TZDM, $K_d$ = 0.13 nM),[19] showing comparable binding affinities to PIB ($K_i$ = 0.44 nM). Consequently, **1a**, **1b**, and **1c** showed 1.20, 0.49, and 0.16 nM binding affinities, respectively. Subsequently, another binding study using AD brain homogenate was attempted for **1b**, **1c**, and the corresponding pure enantiomers in terms of the $IC_{50}$ value. The six compounds of this study showed 13-15 nM binding with narrow differences as well as higher binding than florbetaben ($IC_{50}$ = 24 nM). This also indicated that the chirality of the 3-fluoro-2-hydroxypropyl substituent has little effect on the binding to Aβ plaque. As a consequence of these binding studies, **1b** and **1c** were found to have comparable affinity to PIB, and approximately 1.7-fold higher affinity than florbetaben. The binding affinity of **1a** was relatively low and more lipophilic than **1b** and **1c**. In this regard, **1a** was excluded from further study.

**Table 1**

Binding affinities to Aβ plaque.

| compound | $A\beta_{1-42}$ fibril ($K_i$, nM)[a] | Brain homogenate ($IC_{50}$, nM)[b] |
|---|---|---|
| PIB | 0.44 | -[c] |
| Florbetaben | -[c] | 24 |
| **1a** | 1.20 | -[c] |
| **1b** | 0.49 | 13 |
| (*R*)-**1b** | -[c] | 15 |
| (*S*)-**1b** | -[c] | 14 |
| **1c** | 0.16 | 13 |
| (*R*)-**1c** | -[c] | 14 |
| (*S*)-**1c** | -[c] | 13 |

[a] performed at the Asan Medical Center.

[b] performed by Bayer Healthcare.

[c] not determined.



### 2.3. [$^{18}$F]Radiofluorination and biodistribution study

In vivo distribution studies were conducted with normal mice to obtain the brain uptake level and brain washout abilities of the F-18 labeled compounds. In the first place, a cerebrum/cerebellum kinetics study was carried out using microPET image acquisition and data analysis, giving the time-activity curves. The [$^{18}$F]fluorinated PET tracers were prepared in a

two-step synthesis from the methanesulfonate precursors **19b** and **19c**. Nucleophilic displacement with in situ prepared [$^{18}$F]TBAF in *t*-amyl alcohol solvent,[19] and subsequent deprotection with 1 N HCl afforded [$^{18}$F]**1b** and [$^{18}$F]**1c** in 17% and 40% decay-corrected radiochemical yields (RCYs) after HPLC purification. Dynamic microPET images of the mice were acquired for 70 min and the regions of interest (ROIs) were drawn in the cerebrum and cerebellum brain, and measured as a percentage of the injected dose (%ID). For comparison, [$^{11}$C]PIB and [$^{18}$F]florbetaben were also synthesized using the procedures reported elsewhere,[4,14] and microPET images were obtained under the same conditions. Table 2 summarizes the results of the cerebrum kinetics using four PET tracers. The activity uptake into the brain reached the peak within 1 min in all cases. The peak time of [$^{11}$C]PIB was fastest at 18 seconds, and [$^{18}$F]florbetaben showed a peak time of 35 seconds. The peak times of [$^{18}$F]**1b** and [$^{18}$F]**1c** were 30 and 45 seconds, respectively. The activity amounts in the brain at the peak time of [$^{18}$F]**1b** and [$^{18}$F]**1c** were 22.4 and 11.1 %ID, respectively, which are higher than [$^{11}$C]PIB (7.0 %ID). After the peak time, [$^{18}$F]**1b** and [$^{18}$F]**1c** were washed out rapidly from the brain. The washout ratios of the new PET tracers were 10.2 and 11.8 for [$^{18}$F]**1b**, and 11.1 and 13.9 for [$^{18}$F]**1c** at peak/30 min and peak/60 min, respectively. Although those values were lower than [$^{11}$C]PIB, they were approximately 2.1-2.3 times higher than [$^{18}$F]florbetaben. In the case of [$^{18}$F]**1b**, a biodistribution study was performed using normal mice (n = 3). The %ID/g values of 19 different organs or tissues were measured at 2, 5, 30, 60, and 240 min after being sacrificed (see supplementary data, Table S1). The initial brain uptake was 4.55 %ID/g, and the ratios of 2 min/30 min and 2 min/60 min were 4.6 and 6.1, respectively. This result was consistent with those of the microPET-cerebrum kinetics study (7.5 and 8.7, at 2 min/30 min and 2 min/60 min,

respectively), even though there was a slight difference, presumably due to the different experimental methods.

**Table 2**

Mice cerebrum kinetics

| Compound | ID% | | | | Peak/ 30 min | Peak/ 60 min |
|---|---|---|---|---|---|---|
| | Peak (sec) | 2 min | 30 min | 60 min | | |
| [$^{11}$C]PIB | 7.0 (18) | 4.1 | 0.4 | 0.3 | 17.5 | 23.3 |
| [$^{18}$F]Florbetaben | 17.6 (35) | 15.8 | 3.6 | 3.3 | 4.9 | 5.3 |
| [$^{18}$F]**1b** | 22.4 (30) | 16.5 | 2.2 | 1.9 | 10.2 | 11.8 |
| [$^{18}$F]**1c** | 11.1 (45) | 6.5 | 1.0 | 0.8 | 11.1 | 13.9 |

Further evaluation with enantiomerically pure F-18 labeled (*R*)- and (*S*)-PET tracers was conducted by repeating the aforementioned process. A MicroPET study was performed with normal mice to determine the cerebrum kinetics. The radioactivity changes in the ROI of the brain were measured and time-activity curves in the cerebrum region were obtained (Figure 3). Surprisingly, each enantiomer exhibited largely different brain washout results. Figure 3 shows that the %ID of remaining activity of (*R*) are much higher than that of (*S*) forms in both [$^{18}$F]**1b** and [$^{18}$F]**1c**. Although the initial brain uptake of the (*S*)-PET tracers was slightly higher than the (*R*)-PET tracers, as much as 21% and 13%, respectively, the washout abilities of the (*S*)-PET tracers were superior to those of the (*R*)- PET tracers. The ratios of peak/30 min of (*S*)-PET tracers was 2.8-fold ([$^{18}$F]**1b**) and 4.0-fold ([$^{18}$F]**1c**) higher than those of the corresponding (*R*)-PET tracers. Moreover, the difference in the ratios at 60 min between the (*S*)-PET and (*R*)-PET tracers increased up to 3.0 and 5.2 fold. A biodistribution study was performed with two

enantiomerically pure (*R*)-[$^{18}$F]**1c** and (*S*)-[$^{18}$F]**1c** to confirm the difference in the brain washout abilities using the same procedure as that for the [$^{18}$F]**1b** racemate mentioned above. The initial uptake of (*S*)-[$^{18}$F]**1c** at 2 min was 3.32 %ID/g, which is 11% higher than (*R*)-[$^{18}$F]**1c**. This is consistent with the results of a microPET study. The rate of washout from the brain of (*S*)-[$^{18}$F]**1c** was much larger than (*R*)-[$^{18}$F]**1c**, resulting in 6.1, 12.8, and 23.7 at 2 min/30 min, 2 min/60 min, and 2 min/120 min, respectively. These washout ratios of (*S*)-[$^{18}$F]**1c** were 2.8, 5.6, and 6.5 times higher than those of (*R*)-[$^{18}$F]**1c** at 30 min, 60 min, and 120 min, respectively. Therefore, the washout profile of the *R*/*S* racemates [$^{18}$F]**1b** and [$^{18}$F]**1c** was obtained as the combined result of (*R*) and (*S*)-PET tracers.

**Table 3**

Mice cerebrum kinetics of (*R*)- and (*S*)-PET tracers

| Compound | %ID | | | | Peak/ | peak/ |
|---|---|---|---|---|---|---|
| | Peak (sec) | 2 min | 30 min | 60 min | 30 min | 60 min |
| (*R*)-[$^{18}$F]**1b** | 14.3 (45) | 13.5 | 4.0 | 3.8 | 3.6 | 3.8 |
| (*S*)-[$^{18}$F]**1b** | 17.3 (30) | 13.5 | 1.7 | 1.5 | 10.2 | 11.5 |
| (*R*)-[$^{18}$F]**1c** | 19.0 (35) | 9.2 | 3.1 | 3.4 | 6.1 | 5.6 |
| (*S*)-[$^{18}$F]**1c** | 21.4 (16) | 10.9 | 0.88 | 0.74 | 24.3 | 28.9 |

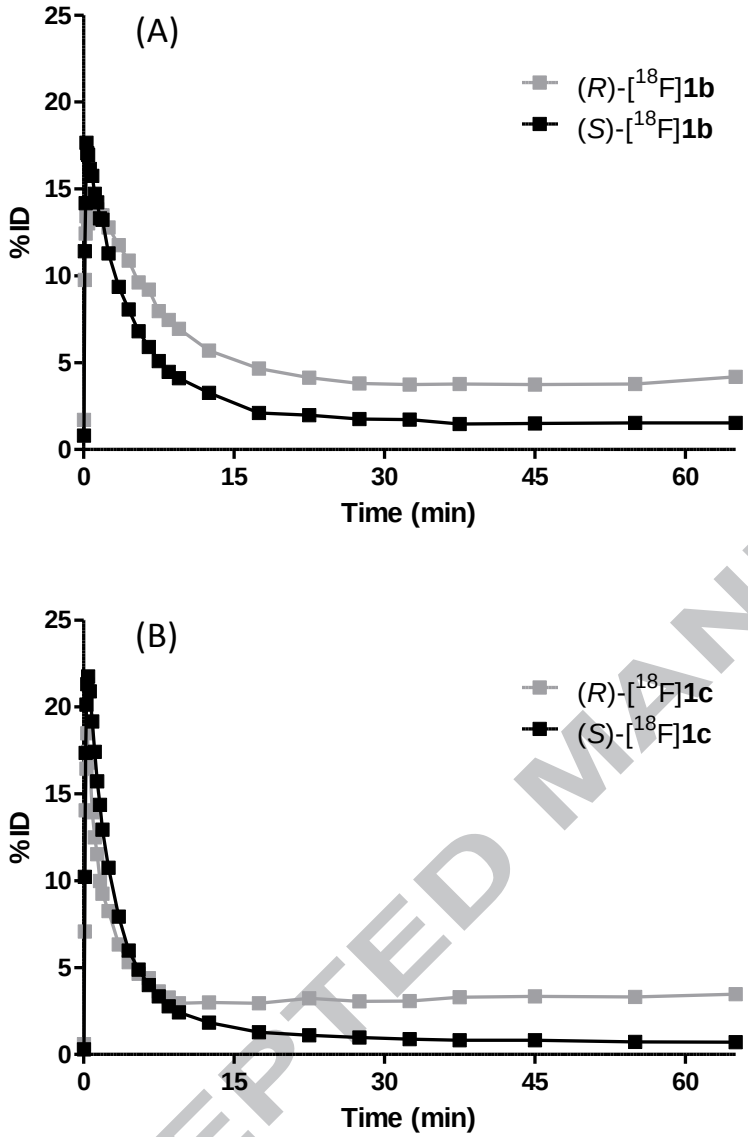


**Figure 3**. Time-activity curves in normal mouse brain. (A) is for [$^{18}$F]**1b**, (B) is for [$^{18}$F]**1c**. Each point is the average of repeated experiments (n = 2 for (*R*)-[$^{18}$F]**1b**, (*S*)-[$^{18}$F]**1b**, and (*R*)-[$^{18}$F]**1c**; n = 4 for (*S*)-[$^{18}$F]**1c**).

In vitro autoradiograms in both AD patient and healthy brain sections were obtained with the [$^{18}$F]**1b** racemate, (*R*)-[$^{18}$F]**1c**, and (*S*)-[$^{18}$F]**1c**. Although the internal regions of the brain (white

matter) exhibited little binding, the Aβ plaque-rich regions of the outer brain (grey matter) were stained well with F-18 labeled PET tracers (Figure 4). In the healthy brain, a binding image was not observed thoroughly. This indicates that new F-18 labeled ligands bind specifically to the Aβ plaque-rich grey matter region of an AD brain.

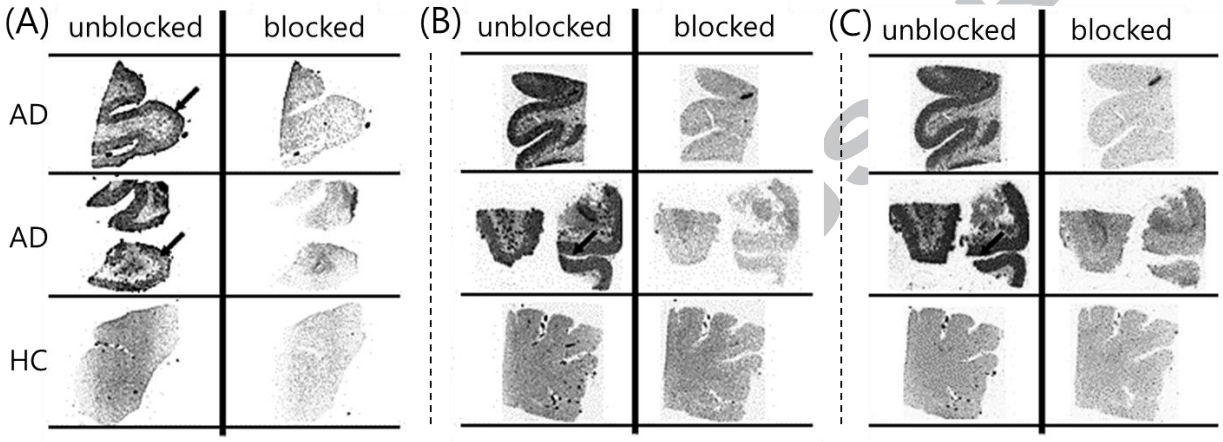


**Figure 4**. In vitro autoradiograms of AD and healthy brain sections stained with F-18 labeled PET tracers. (A) [$^{18}$F]**1b**, (B) (*R*)-[$^{18}$F]**1c**, (C) (*S*)-[$^{18}$F]**1c**, AD: Alzheimer's disease brain, HC: healthy control brain, 'blocked' indicates the use of excess cold substance.

Because (*S*)-[$^{18}$F]**1c** has been found to exhibit the best performance in mice brain pharmacokinetics, it was chosen for further evaluation with healthy rhesus monkeys (n = 2). Two PET images were acquired for 4.5-34 min, and 34-123 min. The left image in Figure 5(A) shows the considerable brain uptake of (*S*)-[$^{18}$F]**1c** in the early period of the scan, whereas the right image indicates that most of the activity has disappeared in monkey brain. The time-activity curve provided clear evidence of the fast washout of (*S*)-[$^{18}$F]**1c** from the frontal cortex after peak uptake at 1.83 min. The ratio of peak/30 min, 60 min, 90 min, and 120 min was 7.0, 16.0,

30.0, and 49, respectively. This washout result in monkeys is superior to most previously reported F-18 labeled PET tracers for Aβ imaging. The change in radioactivity in the cerebellum, a reference region for non-specific binding, showed a similar curve pattern to the frontal cortex (see supplementary data), indicating that there are very little non-specific interactions. The time-activity curve in the white matter region revealed remarkable short retention compared to other lipophilic Aβ-targeting PET tracers, which maintained long retention during scan time. The washout ratio in the white matter was 2.7, 5.6, 9.6, and 16.5 at 30, 60, 90, 120 min, respectively, compared to the peak time (2.33 min, SUV(%)=76.9). This is a similar washout pattern to the grey matter region with a gentle slope.

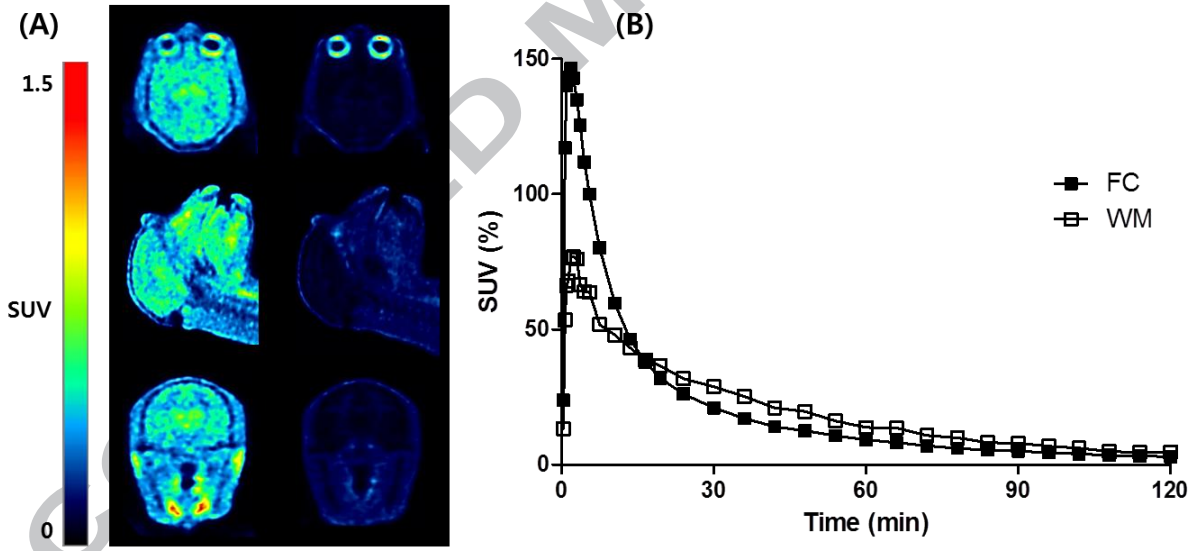


**Figure 5**. PET study with a rhesus monkey. (A) (*S*)-[$^{18}$F]**lc**-PET image of the rhesus monkey; transverse, sagittal, coronal (from top to bottom). The left image was acquired for 4.5-34 min while the right image was acquired for 34-123 min. (B) Time- activity curve. FC: frontal cortex, WM: white matter.

Thus far, there have been a few reports of the use of $^{18}$F-labeled stereoisomers for the diagnosis of brain diseases, such as neuroinflammation (GE180, binding to translocator protein)[20] and Alzheimer's disease (THK5351, binding to the tau protein)[21]. Each single stereoisomer was found to have better brain pharmacokinetics than the opposite stereoisomer as well as the racemate mixture. (*S*)-[$^{18}$F]**1c** also showed better performance than (*R*)-[$^{18}$F]**1c** and the racemate for imaging Aβ plaque. Further evaluation of (*S*)-[$^{18}$F]**1c** and a comparison study of (*R*)- and (*S*)-PET tracers in humans is being investigated.

## 3. Conclusion

The introduction of a 3-[$^{18}$F]fluoropropyl group to the molecules of interest has been a common strategy in the development of F-18 labeled PET tracers until now. The 3-[$^{18}$F]fluoropropyl group, however, plays a role in increasing the lipophilicity of the molecules, resulting in poor pharmacokinetic properties as well as undesired non-specific interactions. To reduce the lipophilicity of the molecules, a hydroxyl group and a nitrogen atom to 3-[$^{18}$F]fluoropropyl and aromatic ring, respectively. In this regard, 3-[$^{18}$F]fluoro-2-hydroxypropyl substituted benzo[*b*]thiophene, and benzo[*d*]thiazoles were synthesized and evaluated for the imaging of Aβ plaque in the brain. All compounds exhibited high binding affinities, and a specific binding profile to Aβ plaque, which was confirmed by in vitro autoradiography with sections of postmortem AD and healthy brains, showing the specific staining of the outer AD brain region. The R/S racemate compounds exhibited improved brain washout properties compared to 3-[$^{18}$F]fluoropropyl substituted molecules. Thereafter, the corresponding (*R*)- and (*S*)-enantiomers were prepared and evaluated by an in vitro binding study and in vivo

pharmacokinetics study. The binding ability of the (*R*) and (*S*) compounds to the AD brain homogenate was similar. Intriguingly, the (*S*)-configured compounds, (*S*)-[$^{18}$F]**1b** and (*S*)-[$^{18}$F]**1c**, showed a significantly higher brain washout ratio (2.9 and 3.9-fold, respectively) than the corresponding (*R*)-configured compounds, giving a peak/30 min ratio of 10.2 and 23.4, respectively. Further evaluation of (*S*)-[$^{18}$F]**1c** with the PET imaging of healthy rhesus monkeys resulted in rapid clearance from the frontal cortex region and moderate clearance in the white matter region. A clinical PET study using (*S*)-[$^{18}$F]**1c** is currently being investigated in South Korea under IND approval by the Korea Ministry of Food and Drug Safety (MFDS). This study is planned to be extended to humans to confirm the different brain pharmacokinetics between (*R*)- and (*S*)-[$^{18}$F]**1c**.

## 4. Experimental

### 4.1. Chemistry

#### 4.1.1. General methods.

All chemicals were obtained from commercial suppliers and were used without further purification unless otherwise stated. Analytical thin layer chromatography (TLC) was performed with Merck silica gel F-254 glass-backed plates. Visualization on TLC was monitored by UV light (254 nm and 365 nm) and phosphomolybdic acid indicator. Column chromatography was carried out using Merck silica gel 60 (230-400 mesh) and eluting with ethyl acetate/hexanes or methanol/dichloromethane. $^{1}$H and $^{13}$C NMR spectra were recorded using either a Varian Gemini-2000 (200 MHz), 400MR (400 MHz), and an INOVA-500 (500 MHz) and calibrated using residual undeuterated solvent or tetramethylsilane as an internal reference. Low resolution mass spectra were obtained using Electrospray Ionization (ESI, Varian 500-MS) and Electron Ionization (EI, Agilent-5973N). High resolution mass spectra were performed at Korea Basic

Science Institute (Daegu, Korea) using Jeol-JMS 700. Melting points were checked using OptiMelt apparatus. Optical rotations were measured at the sodium D line with a 100 mm path length cell by AUTOPOL I Automatic Polarimeter (Rudolph Research Analytical), and reported as follows: $[a]_D^T$ concentration (g/100 mL), and solvent. High performance liquid chromatography (HPLC) was conducted to determine racemate and pure (*R*)- and (*S*)-enantiomer using ChiralPak IA column (Daicel) (4.6 mm x 250 mm). Varian 920LC was used for FC113 compounds under following conditions; isocratic, 0.1% diethylamine in MeOH (100%), 1.0 mL/min, 254 nm (retention time = 9.71 min (FC113R), 10.55 min (FC113S). Varian Prostar 210 was used for FC119 compounds under following conditions; isocratic, 0.1% diethylamine in THF: 0.1% diethylamine in hexane (25:75), 1.0 mL/min, 254 nm (retention time = 17.6 min (FC119R), 20.1 min (FC119S).

[$^{18}$F]Fluoride was produced by the $^{18}$O(p,n)$^{18}$F reaction using [$^{18}$O]water and cyclotron (IBA Cyclone 18/9, Belgium). The progress of [$^{18}$F]fluorination and deprotection was monitored by visualization of radioactivity on TLC using AR-2000 TLC Imaging Scanner (Bioscan). HPLC analysis and purification were performed using Varian Prostar 210 and Nucleosil C18 column (10 mm x 250 mm).

**4.1.2. 2-[4-(*N*-Methyl-*N*-Boc-amino)phenyl]-6-[(2,2-dimethyl-1,3-dioxolan-4-yl)methyloxy]benzo[*b*]thiophene (16a)**

2-[4-(*N*-Methyl-*N*-Boc-amino)phenyl]-6-hydroxylbenzo[*b*]thiazole (**7a**, 200 mg, 0.563 mmol), (2,2-dimethyl-1,3-dioxolan-4-yl)methyl methanesulfonate (**15**, prepared by methanesulfonylation of (2,2-dimethyl-1,3-dioxolan-4-yl)methanol, 177 mg, 0.844 mmol), and $Cs_2CO_3$ (550 mg, 1.69 mmol) were placed in a round-bottom flask, and then DMF (15 mL) was added. The mixture was suspended at 100 °C for 1 h and cooled to room temperature. After the addition of cold water, the aqueous phase was extracted with EtOAc (30 mL x 4), and the

combined organic phase was washed with 0.2 M $NH_4Cl$ aqueous solution (30 mL), brine (30 mL x 2) and dried over $Na_2SO_4$, and then concentrated under reduced pressure. The crude product was purified by flash column chromatography to give **16a** (217 mg, 82%) as a white solid: m.p. 116 °C; $^1$H NMR (400 MHz, $CDCl_3$) δ 1.42 (s, 3H), 1.48 (s, 9H), 1.49 (s, 3H), 3.29 (s, 3H), 3.94 (dd, *J* = 8.6, 5.8 Hz, 1H), 4.00 (dd, *J* = 9.4, 5.8 Hz, 1H), 4.13 (dd, *J* = 9.2, 5.6 Hz, 1H), 4.20 (dd, *J* = 8.4, 6.4 Hz, 1H), 4.53 (quint, *J* = 5.8 Hz, 1H), 7.00 (dd, *J* = 8.8, 2.4 Hz, 1H), 7.28 (d, *J* = 8.8 Hz, 2H), 7.31 (d, *J* = 2.4 Hz, 1H), 7.42 (s, 1H), 7.60-7.65 (m, 3H); $^{13}$C NMR (100 MHz, $CDCl_3$) δ 25.4, 26.8, 28.3, 37.2, 66.8, 69.3, 74.0, 80.6, 105.8, 109.8, 114.8, 118.8, 124.2, 125.6, 126.3, 131.3, 135.1, 140.8, 141.3, 143.4, 154.6, 156.3. HRMS (FAB) m/z: Calcd for $C_{26}H_{31}NO_5S$ $[M]^+$ 469.1923. Found, 469.1920.

**4.1.3. 2-[2-(*N*-Methyl-*N*-Boc-amino)pyridin-5-yl]-6-[(2,2-dimethyl-1,3-dioxolan-4-yl)methyloxy]benzo[*b*]thiophene (16b)**

White solid; yield (206 mg, 87%). m.p. 118 °C; $^1$H NMR (400 MHz, $CDCl_3$) δ 1.42 (s, 3H), 1.48 (s, 3H), 1.55 (s, 9H), 3.44 (s, 3H), 3.93 (dd, *J* = 8.4, 6.0 Hz, 1H), 4.00 (dd, *J* = 9.4, 5.8 Hz, 1H), 4.12 (dd, *J* = 9.6, 5.2 Hz, 1H), 4.19 (dd, *J* = 8.4, 6.4 Hz, 1H), 4.52 (quint, *J* = 5.9 Hz, 1H), 7.00 (dd, *J* = 8.0, 2.4 Hz, 1H), 7.30 (d, *J* = 2.0 Hz, 1H), 7.41 (s, 1H), 7.64 (d, *J* = 8.8 Hz, 1H), 7.77 (d, *J* = 8.4 Hz, 1H), 7.85 (dd, *J* = 8.8, 2.4 Hz, 1H), 8.66 (d, *J* = 2.4 Hz, 1H); $^{13}$C NMR (100 MHz, $CDCl_3$) δ 25.4, 26.8, 28.3, 34.2, 66.8, 69.2, 74.0, 81.4, 105.8, 109.8, 115.0, 118.6, 119.4, 124.3, 125.8, 134.2, 134.8, 137.9, 140.8, 144.5, 154.2, 154.4, 156.5. HRMS (FAB) m/z: Calcd for $C_{25}H_{30}N_2O_5S$ $[M+H]^+$ 471.1954. Found, 471.1952.

**4.1.4. 2-[2-(*N*-Methyl-*N*-Boc-amino)pyridin-5-yl]-6-[(2,2-dimethyl-1,3-dioxolan-4-yl)methyloxy]benzo[*d*]thiazole (16c)**

White solid; yield (388 mg, 92%). m.p. 154 °C; $^{1}$H NMR (400 MHz, $CDCl_3$) δ 1.40 (s, 3H), 1.46 (s, 3H), 1.54 (s, 9H), 3.45 (s, 3H), 3.92 (dd, *J* = 8.6, 5.8 Hz, 1H), 4.00 (dd, *J* = 9.4, 5.8 Hz, 1H), 4.10 (dd, *J* = 9.4, 5.4 Hz, 1H), 4.18 (dd, *J* = 8.6, 6.2 Hz, 1H), 4.50 (quint, *J* = 5.8 Hz, 1H), 7.09 (dd, *J* = 8.8, 2.8 Hz, 1H), 7.34 (d, *J* = 2.8 Hz, 1H), 7.90 (dd, *J* = 8.8, 6.0 Hz, 2H), 8.22 (dd, *J* = 8.8, 2.4 Hz, 1H), 8.94 (d, *J* = 2.6 Hz, 1H); $^{13}$C NMR (100 MHz, $CDCl_3$) δ 25.3, 26.8, 28.3, 34.1, 66.7, 69.4, 73.9, 81.7, 105.1, 109.8, 116.1, 118.2, 123.6, 124.9, 135.1, 136.0, 146.0, 148.8, 154.0, 156.4, 156.8, 162.4. HRMS (FAB) m/z: Calcd for $C_{24}H_{29}N_3O_5S$ $[M+H]^+$ 472.1906. Found, 472.1903.

**4.1.5. 2-[4-(*N*-Methyl-*N*-Boc-amino)phenyl]-6-(2,3-dihydroxypropoxy)benzo[*b*]thiophene (17a)**

Dowex 50WX2 resin (hydrogen form, 250 mg) was added to a solution of 2-[4-(*N*-methyl-*N*-Boc-amino)phenyl]-6-[(2,2-dimethyl-1,3-dioxolan-4-yl)methyloxy]benzo[*b*]thiophene (**16a**, 200 mg, 0.426 mmol) in 10% $H_2O$/MeOH (10 mL). The mixture was suspended at 40 °C for 24 h, and then filtered with a syringe filter equipped with polyethylene frit. After the filtered resin was washed with MeOH, the combined organic solution was concentrated under reduced pressure. Column chromatography was performed to give **17a** (105 mg, 58%) as a white solid: m.p. 167 °C; $^{1}$H NMR (400 MHz, MeOH-$d_4$) δ 1.46 (s, 9H), 3.25 (s, 3H), 3.67 (dd, *J* = 11.4, 5.4 Hz, 1H), 3.72 (dd, *J* = 11.4, 5.0 Hz, 1H), 3.99-4.05 (m, 2H), 4.12 (dd, *J* = 9.0, 3.8 Hz, 1H), 4.89 (br s, 2H), 7.02 (dd, *J* = 8.8, 2.4 Hz, 1H), 7.28 (d, *J* = 8.8 Hz, 2H), 7.41 (d, *J* = 2.4 Hz, 1H), 7.53 (s, 1H), 7.65-7.68 (m, 3H); $^{13}$C NMR (100 MHz, MeOH-$d_4$) δ 27.2, 36.4, 62.8, 69.3, 70.4, 80.5, 105.3, 114.6, 118.9, 124.0, 125.8, 125.9, 131.9, 135.0, 140.5, 140.8, 143.1, 155.0, 157.0. HRMS (FAB) m/z: Calcd for $C_{23}H_{27}NO_5S$ $[M]^+$ 429.1610. Found, 429.1612.

**4.1.6. 2-[2-(*N*-Methyl-*N*-Boc-amino)pyridin-5-yl]-6-(2,3-dihydroxypropoxy)benzo[*b*]thiophene (17b)**

White solid; yield (94 mg, 52%). m.p. 140 °C (decomposed); $^1$H NMR (200 MHz, $CDCl_3$) δ 1.55 (s, 9H), 3.43 (s, 3H), 3.77 (dd, *J* = 11.4, 4.6 Hz, 1H), 3.87 (dd, *J* = 11.4, 3.6 Hz, 1H), 4.07-4.15 (m, 3H), 6.98 (dd, *J* = 8.8, 2.2 Hz, 1H), 7.29 (d, *J* = 2.2 Hz, 1H), 7.39 (s, 1H), 7.62 (d, *J* = 8.8 Hz, 1H), 7.74 (d, *J* = 8.8 Hz, 1H), 7.84 (dd, *J* = 8.6, 2.4 Hz, 1H), 8.64 (d, *J* = 2.6 Hz, 1H); $^{13}$C NMR (100 MHz, $CDCl_3$) δ 28.3, 34.2, 63.6, 69.6, 70.4, 81.5, 105.9, 114.8, 118.7, 119.4, 124.3, 125.9, 134.2, 134.9, 137.9, 140.9, 144.5, 154.3, 154.4, 156.4. HRMS (FAB) m/z: Calcd for $C_{22}H_{26}N_2O_5S$ $[M+H]^+$ 431.1641. Found, 431.1644.

**4.1.7. 2-[2-(*N*-Methyl-*N*-Boc-amino)pyridin-5-yl]-6-(2,3-dihydroxypropoxy)benzo[*d*]thiazole (17c)**

White solid; yield (188 mg, 58%). m.p. 181 °C; $^1$H NMR (400 MHz, DMSO-$d_6$) δ 1.49 (s, 9H), 3.35 (s, 3H), 3.49 (t, *J* = 5.6 Hz, 2H), 3.82-3.89 (m, 1H), 3.97 (dd, *J* = 9.8, 6.2 Hz, 1H), 4.10 (dd, *J* = 9.8, 4.2 Hz, 1H), 4.74 (t, *J* = 5.6 Hz, 1H), 5.05 (d, *J* = 5.2 Hz, 1H), 7.14 (dd, *J* = 9.2, 2.4 Hz, 1H), 7.70 (d, *J* = 2.4 Hz, 1H), 7.86 (d, *J* = 8.8 Hz, 1H), 7.93 (d, *J* = 8.8 Hz, 1H), 8.29 (dd, *J* = 9.2, 2.4 Hz, 1H), 8.94 (dd, *J* = 2.6, 0.8 Hz, 1H); $^{13}$C NMR (100 MHz, DMSO-$d_6$) δ 28.2, 34.2, 63.1, 70.4, 70.7, 81.8, 105.9, 116.8, 118.6, 123.8, 124.9, 135.7, 136.3, 145.8, 148.2, 153.7, 156.2, 157.5, 161.8. HRMS (FAB) m/z: Calcd for $C_{21}H_{25}N_3O_5S$ $[M+H]^+$ 432.1593. Found, 432.1595.

**4.1.8. 2-[4-(*N*-Methyl-*N*-Boc-amino)phenyl]-6-(3-methanesulfonyloxy-2-hydroxypropoxy)benzo[*b*]thiophene (18a)**

After 2-[4-(*N*-methyl-*N*-Boc-amino)phenyl]-6-(2,3-dihydroxypropoxy)benzo[*b*]thiophene (**17a**, 180 mg, 0.419 mmol) and diisopropylethylamine (DIPEA, 0.088 mL, 0.503 mmol) were dissolved in dichloromethane (13 mL) and cooled to -10 °C, MsCl (0.036 mL, 0.461 mmol) was slowly added. The mixture was stirred at -10 °C for 30 min, and water (30 mL) was added. The organic phase was separated, and the aqueous phase was extracted with dichloromethane (30 mL

x 4). The combined organic phase was dried over $Na_2SO_4$, and then concentrated under reduced pressure. The crude product was purified by flash column chromatography to give **18a** (103 mg, 48%) as a white solid: m.p. 155 °C; $^1$H NMR (200 MHz, $CDCl_3$) δ 1.48 (s, 9H), 3.09 (s, 3H), 3.29 (s, 3H), 4.12 (d, *J* = 5.2 Hz, 2H), 4.30-4.34 (m, 1H), 4.43-4.47 (m, 2H), 6.97 (dd, *J* = 8.8, 2.6 Hz, 1H), 7.26-7.31 (m, 3H), 7.41 (s, 1H), 7.59-7.66 (m, 3H); $^{13}$C NMR (100 MHz, $CDCl_3$) δ 28.3, 37.1, 37.6, 68.2, 69.3, 70.2, 80.7, 106.0, 114.6, 118.8, 124.3, 125.6, 126.3, 131.2, 135.4, 140.8, 141.7, 143.5, 154.6, 155.8. HRMS (FAB) m/z: Calcd for $C_{24}H_{29}NO_7S_2$ $[M]^+$ 507.1385. Found, 507.1386.

**4.1.9. 2-[2-(*N*-Methyl-*N*-Boc-amino)pyridin-5-yl]-6-(3-methanesulfonyloxy-2-hydroxypropoxy)benzo[*b*]thiophene (18b)**

White solid; yield (67 mg, 62%). m.p. 146 °C; $^1$H NMR (400 MHz, $CDCl_3$) δ 1.55 (s, 9H), 2.78 (br s, 1H), 3.10 (s, 3H), 3.44 (s, 3H), 4.15 (d, *J* = 5.2 Hz, 2H), 4.35 (m, 1H), 4.44 (dd, *J* = 11.2, 5.6 Hz, 1H), 4.50 (dd, *J* = 11.0, 4.2 Hz, 1H), 7.00 (dd, *J* = 8.8, 2.4 Hz, 1H), 7.32 (d, *J* = 1.6 Hz, 1H), 7.43 (s, 1H), 7.67 (d, *J* = 8.8 Hz, 1H), 7.78 (d, *J* = 8.8 Hz, 1H), 7.86 (dd, *J* = 8.8, 2.8 Hz, 1H), 8.67 (d, *J* = 2.4 Hz, 1H); $^{13}$C NMR (100 MHz, $CDCl_3$) δ 28.2, 34.2, 37.6, 68.3, 68.4, 70.2, 81.5, 106.0, 114.8, 118.7, 119.4, 124.5, 125.8, 134.3, 135.2, 138.3, 140.9, 144.5, 154.3, 154.5, 156.0. HRMS (FAB) m/z: Calcd for $C_{23}H_{28}N_2O_7S_2$ $[M+H]^+$ 509.1416. Found, 509.1412.

**4.1.10. 2-[2-(*N*-Methyl-*N*-Boc-amino)pyridin-5-yl]-6-(3-methanesulfonyloxy-2-hydroxypropoxy)benzo[*d*]thiazole (18c)**

White solid; yield (430 mg, 77%). m.p. 134 °C; $^1$H NMR (200 MHz, $CDCl_3$) δ 1.62 (s, 9H), 3.04 (d, *J* = 5.2 Hz, 1H), 3.17 (s, 3H), 3.53 (s, 3H), 4.21 (d, *J* = 4.6 Hz, 2H), 4.41-4.46 (m, 1H), 4.51-4.58 (m, 2H), 7.15 (dd, *J* = 9.1, 2.5 Hz, 1H), 7.42 (d, *J* = 2.2 Hz, 1H), 7.98 (d, *J* = 8.8 Hz, 1H), 8.00 (d, *J* = 8.8 Hz, 1H), 8.31 (dd, *J* = 8.8, 2.4 Hz, 1H), 9.02 (d, *J* = 2.2 Hz, 1H); $^{13}$C NMR

(50 MHz, $CDCl_3$) δ 28.3, 34.1, 37.6, 68.2, 68.6, 70.1, 81.9, 105.3, 115.9, 118.3, 123.8, 124.8, 135.2, 136.1, 146.1, 149.1, 154.1, 156.2, 156.5, 162.8. HRMS (FAB) m/z: Calcd for $C_{22}H_{27}N_3O_7S_2$ $[M+H]^+$ 510.1369. Found, 510.1367.

**4.1.11. 2-[4-(*N*-Methyl-*N*-Boc-amino)phenyl]-6-[3-methanesulfonyloxy-2-(tetrahydropyran-2-yloxy)propoxy]benzo[*b*]thiophene (19a)**

Dihydropyran (30.7 μL, 0.337 mmol) was added to a solution of **18a** (100 mg, 0.197 mmol) and pyridinium *p*-toluenesulfonate (10 mg, 0.039 mmol) in dichloromethane (3 mL). The mixture was stirred at room temperature for 17 h. After the addition of water (10 mL), the organic phase was separated, and the aqueous phase was extracted with dichloromethane (10 mL x 3). The combined organic phase was dried over $Na_2SO_4$, and then concentrated under reduced pressure. The crude product was purified by flash column chromatography to give **19a** (110 mg, 94%) as a colorless oil: $^1$H NMR (400 MHz, $CDCl_3$) δ 1.48 (s, 9H), 1.56-1.63 (m, 4H), 1.76-1.85 (m, 2H), 3.05 (s, 1.5H), 3.07 (s, 1.5H), 3.29 (s, 3H), 3.52-3.58 (m, 1H), 3.94-3.98 (m, 1H), 4.13-4.21 (m, 1.5H), 4.26-4.34 (m, 1.5H), 4.42 (dd, *J* = 11.2, 2.6 Hz, 0.5H), 4.51 (dd, *J* = 10.8, 4.4 Hz, 0.5H), 4.54-4.60 (m, 1H), 4.84-4.85 (m, 0.5H), 4.86-4.88 (m, 0.5H), 6.98 (dt, *J* = 8.4, 2.6 Hz, 1H), 7.29 (d, *J* = 8.8 Hz, 2H), 7.33 (dd, *J* = 8.4, 2.4 Hz, 1H), 7.42 (s, 1H), 7.61-7.66 (m, 3H); $^{13}$C NMR (100 MHz, $CDCl_3$) δ 19.5, 19.8, 25.2, 25.4, 28.4, 29.7, 30.5, 30.6, 30.7, 37.2, 37.4, 37.5, 37.6, 63.0, 66.8, 67.3, 68.3, 68.4, 69.0, 69.6, 70.2, 72.6, 73.0, 80.6, 94.7, 99.0, 99.3, 105.9, 106.1, 114.6, 114.7, 118.7, 118.8, 124.2, 124.3, 125.6, 126.2, 126.3, 131.2, 131.3, 135.2, 135.3, 135.4, 140.8, 141.4, 141.5, 141.8, 143.4, 143.5, 143.6, 154.6, 155.8, 156.0, 156.1. HRMS (FAB) m/z: Calcd for $C_{29}H_{37}NO_8S_2$ $[M]^+$ 591.1961. Found, 591.1963.

**4.1.12. 2-[4-(*N*-Methyl-*N*-Boc-amino)pyridin-5-yl]-6-[3-methanesulfonyloxy-2-(tetrahydropyran-2-yloxy)propoxy]benzo[*b*]thiophene (19b)**

White solid; yield (103 mg, 75%). m.p. 70 °C; $^1$H NMR (400 MHz, $CDCl_3$) δ 1.55 (s, 9H), 1.57-1.66 (m, 4H), 1.74-1.87 (m, 2H), 3.05 (s, 1.5H), 3.08 (s, 1.5H), 3.44 (s, 3H), 3.54-3.58 (m, 1H), 3.94-3.98 (m, 1H), 4.13-4.22 (m, 1.5H), 4.26-4.35 (m, 1.5H), 4.42 (dd, *J* = 11.0, 5.4 Hz, 0.5H), 4.51 (dd, *J* = 10.8, 4.4 Hz, 0.5H), 4.54-4.57 (m, 1H), 4.83-4.88 (m, 1H), 7.00 (dt, *J* = 8.8, 2.8 Hz, 1H), 7.34 (dd, *J* = 8.2, 2.2 Hz, 1H), 7.44 (s, 1H), 7.67 (d, *J* = 8.4 Hz, 1H), 7.78 (d, *J* = 8.8 Hz, 1H), 7.87 (dd, *J* = 8.8, 2.4 Hz, 1H), 8.68 (dd, *J* = 2.4, 0.6 Hz, 1H); $^{13}$C NMR (100 MHz, $CDCl_3$) δ 19.7, 25.4, 25.5, 28.5, 30.8, 30.9, 34.4, 37.6, 37.7, 63.1, 63.2, 67.0, 67.5, 69.2, 69.9, 72.8, 73.2, 81.7, 99.2, 99.6, 106.1, 106.2, 115.2, 118.9, 119.6, 124.6, 126.0, 126.1, 134.5, 135.1, 135.2, 138.2, 138.3, 141.1, 144.8, 154.5, 154.7, 156.4, 156.5. HRMS (FAB) m/z: Calcd for $C_{28}H_{36}N_2O_8S_2$ $[M+H]^+$ 593.1991. Found, 593.1992.

**4.1.13. 2-[4-(*N*-Methyl-*N*-Boc-amino)pyridin-5-yl]-6-[3-methanesulfonyloxy-2-(tetrahydropyran-2-yloxy)propoxy]benzo[*d*]thiazole (19c)**

White solid; yield (278 mg, 88%). m.p. 62 °C; $^1$H NMR (400 MHz, $CDCl_3$) δ 1.56 (s, 9H), 1.51-1.65 (m, 4H), 1.72-1.85 (m, 2H), 3.06 (s, 1.5H), 3.08 (s, 1.5H), 3.48 (s, 3H), 3.54-3.58 (m, 1H), 3.93-3.98 (m, 1H), 4.14-4.23 (m, 1.5H), 4.27-4.35 (m, 1.5H), 4.43 (dd, *J* = 11.2, 5.2 Hz, 0.5H), 4.49-4.59 (m, 1.5H), 4.84-4.87 (m, 1H), 7.11 (dt, *J* = 9.2, 2.8 Hz, 1H), 7.40 (dd, *J* = 7.4, 2.6 Hz, 1H), 7.92 (d, *J* = 9.2 Hz, 1H), 7.94 (d, *J* = 9.2 Hz, 1H), 8.25 (dd, *J* = 8.8, 2.4 Hz, 1H), 8.97 (d, *J* = 2.4 Hz, 1H); $^{13}$C NMR (100 MHz, $CDCl_3$) δ 19.5, 25.2, 28.2, 30.5, 30.6, 34.1, 37.4, 37.5, 62.9, 67.0, 67.5, 68.9, 69.6, 72.6, 72.9, 81.7, 99.1, 99.3, 105.1, 105.3, 116.0, 118.1, 123.7, 124.7, 124.8, 135.0, 136.1, 146.0, 148.8, 148.9, 154.0, 156.3, 156.4, 156.5, 162.4, 162.5. HRMS (FAB) m/z: Calcd for $C_{27}H_{35}N_3O_8S_2$ $[M+H]^+$ 594.1944. Found, 594.1941.

**4.1.14. 2-[4-(Methylamino)phenyl]-6-(3-fluoro-2-hydroxypropoxy)benzo[*b*]thiophene (1a)**

**19a** (120 mg, 0.203 mmol) and tetra-*n*-butylammonium fluoride (TBAF; 63 mg, 0.243 mmol) were dissolved in *t*-amyl alcohol (3 mL) and stirred at 100 °C for 6 h. After the mixture was cooled to room temperature, the solvent was removed under reduced pressure. Aqueous 4 N HCl (0.55 mL) and THF (2 mL) were added to a reaction vessel, and the mixture was then stirred at 80 °C for 30 min. After cooling to room temperature, water (5 mL) was added and the mixture was then treated with saturated $NaHCO_3$ aqueous solution until basic to litmus. The organic compounds were extracted with EtOAc (5 mL x 4), and the combined organic phase was dried over $Na_2SO_4$, and then concentrated under reduced pressure. The crude product was purified by flash column chromatography to give **1a** (65 mg, 81%) as a light brown solid: m.p. 171 °C; $^1$H NMR (400 MHz, THF-$d_8$) δ 2.79 (d, *J* = 5.2 Hz, 3H), 4.04-4.06 (m, 2H), 4.07-4.15 (m, 1H), 4.50 (dddd, *J* = 47.9, 23.6, 9.2, 4.8 Hz, 2H), 4.69 (d, *J* = 4.8 Hz, 1H), 5.17 (d, *J* = 4.8 Hz, 1H), 6.56 (d, *J* = 8.4 Hz, 2H), 6.92 (dd, *J* = 8.4, 2.4 Hz, 1H), 7.28 (s, 1H), 7.38 (d, *J* = 2.4 Hz, 1H), 7.45 (d, *J* = 8.8 Hz, 2H), 7.54 (d, *J* = 8.8 Hz, 1H); $^{13}$C NMR (100 MHz, THF-$d_8$) δ 30.3, 69.5 (d, *J* = 19 Hz), 69.8 (d, *J* = 7 Hz), 85.3 (d, *J* = 169 Hz), 106.6, 112.6, 115.1, 116.4, 123.4, 124.0, 127.7, 136.5, 140.9, 143.9, 151.0, 157.1. HRMS (FAB) m/z: Calcd for $C_{18}H_{18}FNO_2S$ $[M]^+$ 331.1042. Found, 331.1043.

**4.1.15. 2-[4-(Methylamino)pyridin-5-yl]-6-(3-fluoro-2-hydroxypropoxy)benzo[*b*]thiophene (1b)**

White solid; yield (55 mg, 70%). m.p. 164 °C; $^1$H NMR (400 MHz, DMSO-$d_6$) δ 2.81 (d, *J* = 5.2 Hz, 3H), 3.99-4.04 (m, 2H), 4.05-4.12 (m, 1H), 4.51 (dddd, *J* = 47.6, 19.4, 9.6, 4.2 Hz, 2H), 5.50 (d, *J* = 4.8 Hz, 1H), 6.53 (d, *J* = 8.8 Hz, 1H), 6.84 (q, *J* = 4.7 Hz, 1H), 6.99 (dd, *J* = 8.8, 2.4 Hz, 1H), 7.50 (s, 1H), 7.53 (d, J = 2.0 Hz, 1H), 7.65 (d, *J* = 8.8 Hz, 1H), 7.73 (dd, *J* = 8.8, 2.4 Hz, 1H), 8.35 (d, *J* = 2.8 Hz, 1H); $^{13}$C NMR (100 MHz, DMSO-$d_6$) δ 28.4, 68.1 (d, *J* =

19 Hz), 69.0 (d, *J* = 8 Hz), 84.9 (d, *J* = 167 Hz), 106.6, 108.3, 115.1, 117.1, 118.3, 124.1, 134.6, 135.2, 139.5, 139.7, 145.4, 156.3, 159.5. HRMS (FAB) m/z: Calcd for $C_{17}H_{17}FN_2O_2S$ $[M+H]^+$ 333.1073. Found, 333.1071.

**4.1.16. 2-[4-(Methylamino)pyridin-5-yl]-6-(3-fluoro-2-hydroxypropoxy)benzo[*d*]thiazole (1c)**

White solid; yield (35 mg, 78%). m.p. 180 °C; $^1$H NMR (400 MHz, DMSO-$d_6$) δ 2.88 (d, *J* = 4.8 Hz, 3H), 4.05-4.09 (m, 2H), 4.11-4.16 (m, 1H), 4.55 (dddd, *J* = 47.5, 18.6, 9.6, 4.5 Hz, 2H), 5.55 (d, *J* = 5.2 Hz, 1H), 6.59 (d, *J* = 8.8 Hz, 1H), 7.12 (dd, *J* = 8.8, 2.4 Hz, 1H), 7.25 (q, *J* = 4.5 Hz, 1H), 7.67 (d, *J* = 2.8 Hz, 1H), 7.85 (d, *J* = 8.8 Hz, 1H), 7.98 (dd, *J* = 9.0, 2.6 Hz, 1H), 8.67 (d, *J* = 2.8 Hz, 1H); $^{13}$C NMR (100 MHz, DMSO-$d_6$) δ 28.3, 68.6 (d, *J* = 19 Hz), 69.2 (d, *J* = 7 Hz), 84.9 (d, *J* = 168 Hz), 106.1, 108.3, 116.1, 117.9, 122.9, 135.2, 135.4, 147.8, 148.6, 156.4, 160.9, 164.0. HRMS (FAB) m/z: Calcd for $C_{16}H_{16}FN_3O_2S$ $[M+H]^+$ 334.1026. Found, 334.1027.

**4.1.17. (*R*)-2-[4-(Methylamino)pyridin-5-yl]-6-(3-fluoro-2-hydroxypropoxy)benzo[*b*]thiophene ((*R*)-1b)**

(*R*)-**1b** was synthesized in the same manner as Scheme 1, starting from compound **7b** and (*S*)-(2,2-dimethyl-1,3-dioxolan-4-yl)methyl methanesulfonate ((*S*)-**15**, prepared by methanesulfonylation of (*R*)-2,2-dimethyl-1,3-dioxolane-4-methanol (99% ee, Aldrich)). $[a]_D^{23}$ = -13.3º (1.5, THF); Chiral HPLC analysis, retention time = 10.15 min (>99 ee%).

**4.1.18. (*S*)-2-[4-(Methylamino)pyridin-5-yl]-6-(3-fluoro-2-hydroxypropoxy)benzo[*b*]thiophene ((*S*)-1b)**

(*S*)-**1b** was synthesized in the same manner as Scheme 1, starting from compound **7b** and (*R*)-(2,2-dimethyl-1,3-dioxolan-4-yl)methyl methanesulfonate ((*R*)-**15**, prepared by

methanesulfonylation of (*S*)-2,2-dimethyl-1,3-dioxolane-4-methanol (99% ee, Aldrich)). $[a]_D^{23}$ = +13.3º (1.5, THF); Chiral HPLC analysis, retention time = 11.18 min (>99 ee%)

**4.1.19. (*R*)-2-[4-(Methylamino)pyridin-5-yl]-6-(3-fluoro-2-hydroxypropoxy)benzo[*d*]thiazole ((*R*)-1c)**

(*R*)-**1c** was synthesized in the same manner as Scheme 1, starting from compound **7c** and (*S*)-(2,2-dimethyl-1,3-dioxolan-4-yl)methyl methanesulfonate ((*S*)-**15**, prepared by methanesulfonylation of (*R*)-2,2-dimethyl-1,3-dioxolane-4-methanol (99% ee, Aldrich)). $[a]_D^{23}$ = -9.33º (1.5, THF); Chiral HPLC analysis, retention time = 17.3 min (>99 ee%)

**4.1.20. (*S*)-2-[4-(Methylamino)pyridin-5-yl]-6-(3-fluoro-2-hydroxypropoxy)benzo[*d*]thiazole ((*S*)-1c)**

(*S*)-**1c** was synthesized in the same manner as Scheme 1, starting from compound **7c** and (*R*)-(2,2-dimethyl-1,3-dioxolan-4-yl)methyl methanesulfonate ((*R*)-**15**, prepared by methanesulfonylation of (*S*)-2,2-dimethyl-1,3-dioxolane-4-methanol (99% ee, Aldrich)). $[a]_D^{23}$ = +9.33º (1.5, THF); Chiral HPLC analysis, retention time = 20.6 min (>99 ee%)

**4.2. In Vitro binding study**

**4.2.1. Method 1 (Synthetic $A\beta_{1-42}$ protein aggregate)**

Aβ peptide ($A\beta_{1-42}$, 1 mg, Bachem) was dissolved in 1 mL of DMSO, and diluted with phosphate buffer (pH 7.4, 9 mL). $A\beta_{1-42}$ protein aggregate produced by incubating at 37 °C for 60 min were dispensed in 0.5 mL each and stored in a refrigerator at -80 °C. The $A\beta_{1-42}$ protein aggregate solution (10 nM) was placed in a test tube and [$^{125}$I]TZDM (6-[$^{125}$I]iodo-2-(4-dimethylaminophenyl)benzo[*b*]thiazole) (50 μL, 0.046~5.9 pM) was added. The resulting solution was diluted with 10% ethanol to be a total volume of 1 mL, and subjected to incubation

at room temperature for 3 h. Thereafter, [$^{125}$I]TZDM bound to the A$\beta_{1-42}$ protein aggregate was separated from unbound [$^{125}$I]TZDM using a cell harvester (Brandel M-24R). Gamma radiation was measured using a gamma counter, and then the dissociation constant $K_d$ was calculated, in which non-specific binding was tested using Thioflavin T (ThT, 2 μM). As a result of that, $K_d$ value of [$^{125}$I]TZDM was revealed to be 0.13 nM.

To a test tube, 10% ethanol (0.850 mL), A$\beta_{1-42}$ protein aggregate (50 μL, 10 nM), the respective unlabled ligand of this paper (50 μL, 1 μM) were added in sequence. After [$^{125}$I]TZDM (50 μL, 0.05 nM) was added, the solution stood at room temperature for 3 h. Using a cell harvester (Brandel M-24R), A$\beta_{1-42}$ protein aggregate binding [$^{125}$I]TZDM was separated from free [$^{125}$I]TZDM. Each was measured by a gamma counter, in which non-specific binding was tested using ThT (2 μM).

#### 4.2.2. Method 2 (Brain homogenate)

Brain homogenates were prepared by homogenizing dissected brain of AD patients in PBS buffer solution (pH 7.4) at the concentration of 100 mg wet tissue/mL. Various concentrations of unlabeled ligands of this paper were incubated with 100 mg/mL homogenate and tritiated ligand at room temperature for 3 h. The tritiated ligand bound to homogenates was filtered through Whatman CF/B filters using a cell harvester. The filters containing the bound tritiated ligand were washed with PBS buffer and assayed for radioactivity amount in a gamma counter. The result of inhibition experiments were converted to $IC_{50}$ values through a nonlinear regression analysis.

### 4.3. [$^{18}$F]Radiosynthesis

#### 4.3.1. Radiosynthesis of [$^{18}$F]lb

[$^{18}$F]Fluoride (40 mCi) ion produced by irradiation of [$^{18}$O]$H_2O$ with cyclotron was trapped in a Chromafix® (PS-$HCO_3$) cartridge, and was released into a reactor by elution of a methanol solution (0.7 mL) containing tetra-*n*-butylammonium bicarbonate ($TBAHCO_3$, 0.08 mL). After removing the solvent by azeotropic evaporation with acetonitrile (0.5 mL) at 100 °C while passing nitrogen over the solution. A solution of precursor compound 19b (5 mg) dissolved in tetrahydrofuran (0.05 mL) and *t*-amyl alcohol (1.0 mL) was added to the reactor. After the reaction mixture was heated at 120 °C for 20 min, the solvent was removed by a gentle stream of nitrogen under heating at 100 °C. 1 N HCl aqueous solution (0.5 mL) was added and stirred at 100 °C for 5 min. After cooling to room temperature, the reaction mixture was neutralized by the addition of 2 N NaOH solution (0.25 mL). The crude solution was loaded onto a C18 Sep-Pak cartridge (Waters), and washed with 5 mL of water, and then eluted with 2 mL of acetonitrile into a vial. The acetonitrile solution was injected into HPLC equipped with a semipreparative column. [$^{18}$F]**1b** containing fraction was collected and diluted with 15 mL of water, which was passed through a preconditioned C18 Sep-Pak cartridge. The final product was eluted with 1 mL of ethanol. Radiochemical yield and specific activity of the final product, [$^{18}$F]**1c**, were 16.95% (decay-corrected) and 850 Ci/mmol, respectively. Total synthesis time was 65 min including HPLC purification.

#### 4.3.2. Radiosynthesis of [$^{18}$F]1c

[$^{18}$F]**1c** was prepared by the same procedure as the radiosynthesis of [$^{18}$F]**lb** with 40 mCi of [$^{18}$F]fluoride ion. Radiochemical yield and specific activity were 40.17% (decay-corrected) and >1200 Ci/mmol, respectively. Total synthesis time was 75 min including HPLC purification.

### 4.4. MicroPET image acquisition

An animal PET system (Focus 120 microPET; Concorde Microsystems, Inc.) was used for brain image of normal mice, which were maintained under isoflurane anesthesia during PET image acquisition. 70 min dynamic PET scans were acquired after a tail vein injection of 7.4 MBq (0.20 mCi) of [$^{18}$F]fluorinated ligands of this study. The dynamic imaging sequence was 6x5, 6x15, 8x60, 6x300, and 3x600 s, with 128x128x95 matrices and voxel sized of 0.432x0.432x0.796 mm$^3$. PET images were reconstructed using ordered subset expectation maximization (OSEM) algorithm. Regions of interest (ROIs) were drawn on cerebrum and cerebellum of mice. The same experiment was performed with [$^{11}$C]PIB and [$^{18}$F]Florbetaben for comparison study.

**4.5. Biodistribution study**

Male NMRI mice (26-34 g, n = 3 per time point) were injected with F-18 labeled compounds (150 kBq/100 μL) through a tail vein. The mice were sacrificed by decapitation under isoflurane anesthesia at various time points (2, 5, 30, 60, 90 min for [$^{18}$F]**1b**; 2, 5, 15, 30, 45, 60, 120, 240 min for (*R*)-[$^{18}$F]**1c** and (*S*)-[$^{18}$F]**1c**) post intravenous injection At the same time points, urine and feces were quantitatively collected. Following organs and tissues were removed: spleen, liver, kidney, lung, femur, heart, brain, fat, thyroid, muscle, skin, blood, tail, stomach, testicle, intestine, pancreas, adrenals, cranial bone. The radioactivity of them was measured using a gamma counter. The decay-corrected percentage of injected dose per tissue weight (%ID/g standard deviation) was calculated.

**4.6. Autoradiographical analysis**

Fresh frozen and paraffin-embedded sections of the frontal lobe from Alzheimer's patients as well as age matched healthy controls were used for the study. The paraffin sections were deparaffinized using routine histological methods. The sections were incubated in 25 mM Hepes buffer (pH 7.4, 0.1% BSA, 200 μL/slide) with the F-18 labeled compounds of this study (10 Bq/μL) for 1.5 h at room temperature. Blocking experiments were performed using 1000-fold excess of the unlabeled compounds, which were added to the incubation mixture prepared above. Thereafter, sections were rinsed with Hepes buffer (x4), 40% ethanol (x2), and distilled water (x2). After air-drying, the sections were exposed to Fuji Film imaging plates overnight. Images were obtained using a phosphoimager (Fuji BAS5000).

### 4.7. PET image of rhesus monkey with (*S*)-[$^{18}$F]1c

Two young rhesus monkeys (4.95 and 4.6 kg) were anesthetized with sevoflurane (2-8% in medical air) and treated with (*S*)-[$^{18}$F]**lc** (148 and 161 MBq, respectively) through intravenous injection. Sevoflurane anesthesia was continued throughout the procedure. PET image was acquired using a high-resolution research tomography (HRRT) PET scanner for 123 min, and reconstructed with OP-3D-OSEM with PSF modeling. Regions of interest (ROIs) were drawn on thalamus, temporal cortex, frontal cortex, white matter (centrum semiovale), cerebellum, and whole brain. The ROI data were reanalyzed using coregistered MRI-PET images, and then applied to obtain time-radioactivity (SUV (%)) curves.

### Acknowledgements

The research was supported by the Converging Research Center Program through the Ministry of Science, ICT and Future Planning, Korea (2013K000326 and 2014M3C1A8066306).

**Supplementary data**

Supplementary data associated with this article can be found, in the online version

**References**

1. (a) Hardy, J.; Allsop, D. *Trends Pharmacol. Sci.* **1991**, *12*, 383. (b) Selkoe, D. J. *Neruon* **1991**, *6*, 487. (c) Hardy, J.; Selkoe, D. J. *Science* **2002**, *297*, 353.

2. (a) Nordberg, A.; Rinne, J. O.; Kadir, A.; Långström, B. *Nature Rev. Neurol*. **2010**, *6*, 78. (b) Quigley, H.; Colloby, S. J.; O'Brien, J. T. *Int. J. Geriatr. Psychiatry* **2011**, *26*, 991.

3. (a) Mathis, C. A.; Lopresti, B. J.; Klunk, W. E. *Nucl. Med. Biol*. **2007**, *34*, 809. (b) Johnson, K. A.; Minoshima, S.; Bohnen, N. I.; Donohoe, K. J.; Foster, N. L.; Herscovitch, P.; Karlawish, J. H.; Rowe, C. C.; Carrillo, M. C.; Hartley, D. M.; Hedrick, S.; Pappas, V.; William H. Thies, W. H. *J. Nucl. Med*. **2013**, *54*, 476.

4. (a) Mathis, C. A.; Wang, Y.; Holt, D. P.; Huang, G.-F.; Debnath, M. L.; Klunk, W. E. *J. Med. Chem*. **2003**, *46*, 2740. (b) Klunk, W. E.; Engler, H.; Nordberg, A.; Wang, Y.; Blomqvist, G.; Holt, D. P.; Bergström, M.; Savitcheva, I.; Huang, G.-F.; Estrada, S.; Ausén, B.; Debnath, M. L.; Barletta, J.; Price, J. C.; Sandell, J.; Lopresti, B. J.; Wall, A.; Koivistro, P.; Antoni, G.; Mathis, C. A.; Långström, B. *Ann. Neurol*. **2004**, *55*, 306.

5. Klunk, W. E.; Mathis, C. A. *Curr. Opin. Neurol*. **2008**, *21*, 683.

6. Choi, S. R.; Golding, G.; Zhuang, Z.; Zhang, W.; Lim, N.; Hefti, F.; Benedum, T. E.; Kilbourn, M. R.; Skovronsky, D.; Kung, H. F. *J. Nucl. Med.* **2009**, *50*, 1887.

7. (a) Koole, M.; Lewis, D. M.; Buckley, C.; Nelissen, N.; Vandenbulcke, M.; Brooks, D. J.; Vandenberghe, R.; Van Laere, K. *J. Nucl. Med*. **2009**, *50*, 818. (b) GE β-amyloid agent approved. *J. Nucl. Med*. **2013**, *54*, 10N.

8. Zhang, W.; Oya, S.; Kung, M.-P.; Hou, C.; Maier, D. L.; Kung, H. F. *Nucl. Med. Biol*. **2005**, *32*, 799.

9. Pike, V. W. *Trends Pharmacol. Sci*. **2009**, *30*, 431.

10. (a) Ono, M.; Kawashima, H.; Nonaka, A.; Kawai, T.; Haratake, M.; Mori, H.; Kung, M.-P.; Kung, H. F.; Saji, H.; Nakayama, M. *J. Med. Chem*. **2006**, *49*, 2725. (b) Qu, W.; Kung, M.-P.; Hou, C.; Oya, S.; Kung, H. F. *J. Med. Chem*. **2007**, *50*, 3380. (c) Cai, L.; Cuevas, J.; Temme, S.; Herman, M. M.; Dagostin, C.; Widdowson, D. A.; Innis, R. B.; Pike, V. W. *J. Med. Chem*. **2007**, *50*, 4746. (d) Lee, I.; Choe, Y. S.; Choi, J. Y.; Lee, K.-H.; Kim, B.-T. *J. Med. Chem*. **2012**, *55*, 883.

11. (a) Cai, L.; Lu, S.; Pike, V. W. *Eur. J. Org. Chem*. **2008**, 2853. (b) Schirrmacher, R.; Wängler, C.; Schirrmacher, E. *Mini-Rev. Org. Chem.* **2007**, *4*, 317.

12. (a) Dischino, D. D.; Welch, M. J.; Kilbourn, M. R.; Raichle, M. E. *J. Nucl. Med.* **1983**, *24*, 1030. (b) Waterhouse, R. N. *Mol. Imaging Biol*. **2003**, *5*, 376. (c) Pajouhesh, H.; Lenz, G. R. *NeuroRx*. **2005**, *2*, 541.

13. Johnson, A. E.; Jeppsson, R.; Sandell, J.; Wensbo, D.; Neelissen, J. A. M.; Juréus, A.; Ström, P.; Norman, H.; Farde, L.; Svensson, S. P. S. *J. Neurochem*. **2009**, *108*, 1177.

14. Rowe, C. C.; Ackerman, U.; Browne, W.; Mulligan, R.; Pike, K. L.; O'Keefe, G.; Tochon-Danguy, H.; Chan, G.; Berlangieri, S. U.; Jones, G.; Dickinson-Rowe, K. L.; Kung, H. P.; Zhang, W.; Kung, M. P.; Skovronsky, D.; Dyrks, T.; Holl, G.; Krause, S.; Friebe, M.; Lehman, L.; Lindemann, S.; Dinkelborg, L. M.; Masters, C. L.; Villemagne, V. L. *Lancet Neurol*. **2008**, *7*, 129.

15. Rowe, C. C.; Villemagne, V. L. *J. Nucl. Med*. **2011**, *52*, 1733.

16. Machatha, S. G.; Yalkowsky, S. H. *Int. J. Pharm*. **2005**, *294*, 185.

17. Ho, P.-T. *Tetrahedron Lett*. **1978**, *19*, 1623.

18. (a) Kim, D. W.; Ahn, D.-S.; Oh, Y.-H.; Lee, S.; Kil, H. S.; Oh, S. J.; Lee, S. J.; Kim, J. S.; Ryu, J. S.; Moon, D. H.; Chi, D. Y. *J. Am. Chem. Soc.* **2006**, *128*, 16394. (b) Lee, S. J.; Oh, S. J.; Chi, D. Y.; Kang, S. H.; Kil, H. S.; Kim, J. S.; Moon, D. H. *Nucl. Med. Biol*. **2007**, *34*, 345.

19. Lee, J. H.; Byeon, S. R.; Kim, Y.; Lim, S. J.; Oh, S. J.; Moon, D. H.; Yoo, K. H.; Chung, B. Y.; Kim, D. J. *Bioorg. Med. Chem*. **2008**, 18, 5701.

20. Wadsworth, H.; Jones, P. A.; Chau, W.-F.; Durrant, C.; Fouladi, N.; Passmore, J.; O'Shea, D.; Wynn, D.; Morisson-Iveson, V.; Ewan, A.; Thaning, M.; Mantzilas, D.; Gausemel, I.; Khan, I.; Black, A.; Avory, M.; Trigg, W. *Bioorg. Med. Chem*. **2012**, *22*, 1308.

21. (a) Okamura, N.; Furumoto, S.; Furukawa, K.; Ishiki, A.; Harada, R.; Iwata, R.; Tashiro, M.; Yanai, K.; Arai, H.; Kudo, Y. *J. Nucl. Med.* **2015**, *56* (suppl. 3) 138. (b) Bohnen, N. I. *J. Nucl. Med*. **2015**, *56*(10), 13N.

Graphical Abstract.